Proceedings of Fuelcell2004
The 2nd International Conference on Fuel Cell Science, Engineering and Technology
June 14-16, 2004, Rochester, New York, USA

FUELCELL2004-2465

A SIMPLE THERMAL MODEL OF PEM FUEL CELL STACKS

B. Wetton [1], K. Promislow [2] and A. Çağlar [3]

[1] University of British Columbia, Vancouver, BC, CANADA; E-Mail: wetton@math.ubc.ca
[2] Michigan State University, East Lansing, MI 48824-1027, USA; E-Mail: kpromisl@math.msu.edu
[3] University of British Columbia, Vancouver, BC, CANADA; E-Mail: atife@math.ubc.ca

ABSTRACT

A simple model is developed that determines the temperature distribution through a unit fuel cell with straight flow channels, in steady state operation. Using the large aspect ratio of the typical fuel cell geometry, the thermal model approximately decouples cross-plane thermal transport at each channel location. Using the fact that in-plane thermal conductivities are much larger than through-plane in typical bipolar plate construction, it is possible to further approximate the cross-plane thermal transport with a simple, one-dimensional model. We then consider the thermal coupling of several unit cells connected in series. In this way, we can simulate the effect of an anomalously hot cell in a stack environment. We take as inputs to the model the cell voltage and local current density, membrane resistance and condensation rates from a previously developed model. The thermal model outputs the average coolant temperature and the temperature distribution through the bipolar plates and membrane electrode assembly at each location down the channel. Although we are aware that there are significant coupling effects between the thermal distribution and performance, this is not taken into account in this study.

INTRODUCTION

A Polymer Electrolyte Membrane Fuel Cell is an electrochemical device in which the energy of the chemical reaction is converted directly into electricity. By combining hydrogen fuel with oxygen from air, electricity is formed without combustion of any form. Water and heat are the only by products when hydrogen is used as the fuel source. Further details of general fuel cell operation can be found in Larminie and Dicks (2003).

Computational modeling of fuel cell operation has been seen as a way to perform design optimization more efficiently than by experimental testing in certain situations, just has been undertaken for other technologies, most notably in Aeronautics. Early models of unit cell performance were developed by Springer et al. (1991) and others. A modern version of this kind of low-dimensional averaged model was recently developed by our group (Berg et al., 2004). Recent three-dimensional computational models have been developed (Berning et al, 2001; Dutta et al. 2001; Mazumder and Cole, 2003; and Natarajan and Van Nguyen, 2003). These are 3-D finite volume computational tools that describe the coupled mass transport and electrochemistry in unit cells. The next few years hold the promise of robust, commercially available three-dimensional and transient unit cell codes capable of describing many aspects of fuel cell operation.

A few authors (Nguyen and White, 1993; Djilali and Lu, 2002) have concentrated specifically on computational models of heat transfer in fuel cells. However, there have been few attempts to model the effects of cell-to-cell coupling in a stack environment. In this paper, we develop simple models for the temperature distribution in a unit cell with straight flow channels, in steady state operation. These simple models are then extended to the stack environment. Some preliminary computations show how excess heat from a center hot cell spreads to neighboring cells. The results are of interest in design since temperature increases of even a few degrees at the membrane can lead to thermal runaway: higher temperatures leading to dryer membranes which have lower conductivity and so further increase temperature. However, the coupling of temperature profiles to performance in this way has not yet been done. A further limitation of this study is that at this time, experimental results to validate and fit the model are not yet available.

THE SINGLE CELL MODEL

Our approach is to begin with computational output from our unit cell code (Berg et al., 2004). This code assumes a linear coolant temperature profile between given inlet and outlet coolant temperatures. It also assumes the temperature is locally constant through the MEA. With these assumptions it computes performance (local current and water crossover) based on given operating conditions. This output can be used to predict a nonlinear temperature profile in the cell using the models described below. This can be considered as one step of an iterative procedure.

The following data is used from the unit cell computational model: local current density $i(y)$; cell voltage V; cathode condensation rate $\Gamma(y)$; and membrane area-specific resistivity $R(y)$. Here y is the down-channel coordinate from cathode inlet $(y=0)$ to outlet $(y=L_c)$. The cell length is L_c=0.67m. The other coordinates are through-MEA (membrane electrode assembly) z and cross-channel x. The condensation rate is computed using a difference approximation of

$$\Gamma = \frac{dQ_l}{dy}$$

from the model values of $Q_l(y)$. Note that Q_l and other channel fluxes are given per unit orthogonal distance x. Nomenclature is summarized in a final section of this paper. We use standard conditions for Ballard Mk9 hardware (see Berg et al., 2004) run in counterflow operation to generate the data that is used below. Coolant flows in the direction of the cathode gases. In each unit cell, coolant channels are found between the anode and cathode plates.

We make the following assumptions:

1. Heat is removed from the cell only through the coolant stream (very reasonable for cells away from stack ends).
2. Ohmic heating other than in the membrane is neglected.
3. Thermal effects of the channel gas streams are neglected except condensation in the cathode.
4. We assume the anode channel stream is always under-saturated (so no condensation here).
5. The temperature through the MEA and bipolar plates does not depend on the cross-channel direction x.

It is this last assumption that is the most suspect, although the fact that in-plane thermal conductivities of the bipolar plates and electrodes are much higher than through-plane does make this approximately true. Still, this limits the results to qualitative accuracy only. This assumption along with the first leads to a natural decomposition of the temperature distribution in a fuel cell: we consider the average coolant temperature $T(y)$ and at each y we consider the temperature $\theta(z)$ through the MEA.

We can write a simple model for $T(y)$ based on the assumptions above:

$$cQ_o \frac{dT}{dy} = (V_{TN} - V)i(y) + H_{vap}\Gamma \qquad (1)$$

where V_{TN} =1.28V is the thermal neutral voltage of the Oxygen Reduction Reaction with product of *vapour*; H_{vap} is the heat of vaporization, 45.4 kJ/mole; c is the coolant heat capacity 3.5kJ/kg/ºC; Q_o =0.135 kg/sm is the coolant flux per unit cell per unit width. We use values for operating conditions and material constants provided by experimentalists at Ballard Power Systems for their Mk9 hardware. It is possible to further divide $V_{TN} - V$ into the following losses

$$V_{TN} - V = iR + \eta \qquad (2)$$

where η is the cathode overpotential. The anode overpotential is neglected in this study.

In Fig. 1 we show some coolant temperature profiles computed from this model. The base membrane resistivity we consider has an average of $9.37 \times 10^{-6}\ \Omega\text{-m}^2$ but varies in y due to membrane hydration effects in the unit cell model. Also shown are results for membrane resistance increased by a factor of 2 and 4 (obtained from the unit cell model by reducing the proton diffusivity parameter by these factors). Our original premise that the temperature profile between inlet and outlet is linear appears to be reasonable.

In Fig. 2, we show the relative size of the right hand side terms of Eq.1 for the base resistance case where the first term has been divided as in Eq.2. Condensation does not occur near the inlet since the air is undersaturated at inlet. At outlet there is evaporative cooling since here there is strong water crossover to the under-saturated anode at its inlet (recall, we are considering counterflow operation).

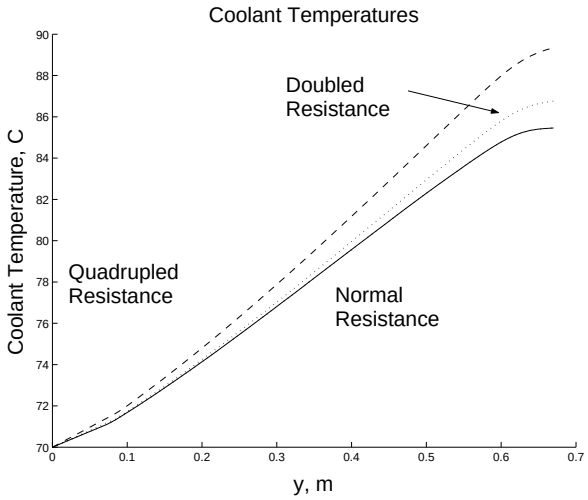

Fig. 1: Predicted coolant temperature $T(y)$ for base membrane resistance (solid line), doubled resistance (dotted), quadrupled resistance (points).

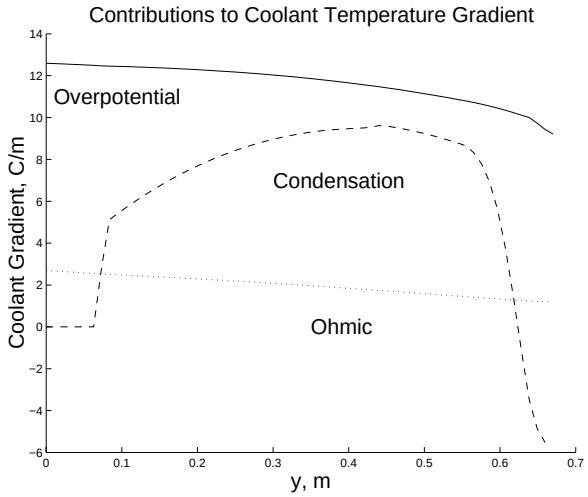

Fig. 2: Relative contribution of coolant heating from over-potential (solid), membrane ohmic loses (dotted) and condensation (points).

Using the coolant temperature $T(y)$ and the unit cell model output we can post-process the temperature distribution $\theta(z)$ through the bipolar plates and the MEA at each y. We make the following additional assumptions:

6. The catalyst layers are idealized to zero thickness.
7. We assume that condensation occurs uniformly in the cathode electrode.
8. At the boundary between coolant channel and the bipolar plate, thermal transfer can be described by the Nusselt number Nu=48/11 for circular channels with uniform heat flux.
9. At the anode, the reaction is endothermic with voltage V_a = -0.25V (this is the voltage equivalent of the anode reaction enthalpy), which translates into a sink of heat in our equations, but kinetic losses are neglected.

This last point deserves some discussion. The work of Lampinen and Famino (1993) shows that stripping off the electrons from hydrogen requires energy (V_a) although the total energy of the Oxygen Reduction Reaction is still given by V_{TN} so an additional, balancing thermal potential of $-V_a$ must be applied at the cathode. Note that there is some controversy in the literature on the value of V_a.

We can parameterize $\theta(z)$ with the values θ_1 in the cathode plate by the coolant, θ_2 at cathode plate/electrode edge, θ_3 at cathode catalyst, θ_4 at anode catalyst and θ_5 at the anode plate/electrode edge. Our single cell is considered to be in the centre of a stack of cells run at identical conditions so it is appropriate to use θ_1 as the temperature of the anode plate by the coolant. See figure 3.

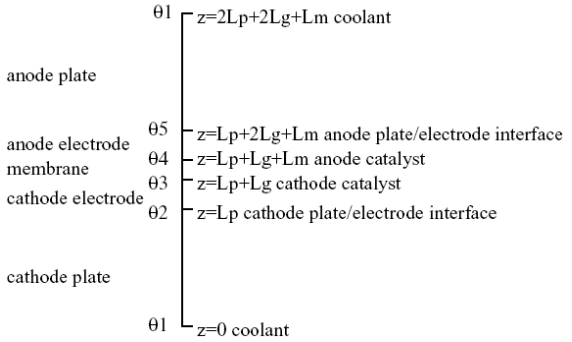

Fig. 3: Domain of the bipolar plates and MEA.

The temperature $\theta(z)$ is linear in the anode and cathode plates, and the anode electrode. Due to the uniform ohmic heating in the membrane we have

$$\kappa_m \theta'' = -\frac{i^2 R}{L_m}$$

and in the cathode electrode we have

$$\kappa_g \theta'' = -\frac{H_{vap}\Gamma}{L_g}$$

due to the uniform condensation. Here, L_m =50 μ is the membrane thickness; L_g =100 μ is the electrode thickness; κ_m =0.56 W/mºC and κ_g =1 W/mºC are the corresponding thermal conductivities. We are now able to determine a piecewise linear/quadratic form for $\theta(z)$ from the 5-vector of reference $\underline{\theta}$ values. We will describe below a system of linear equations for these values. Four conditions arise from thermal balances:

$$\kappa_p \theta' - \kappa_g \theta' = 0 \text{ plate/cathode interface} \quad (3a)$$

$$\kappa_p \theta' - \kappa_g \theta' = 0 \text{ plate/anode interface} \quad (3b)$$

$$\kappa_g \theta' - \kappa_m \theta' = U_a i \text{ anode catalyst} \quad (4)$$

$$\kappa_g \theta' - \kappa_m \theta' = (\eta - U_a) i \text{ cathode catalyst} \quad (5)$$

where the derivatives above are taken as the appropriate one-sided ones.

We describe the fifth condition, the thermal balance into the coolant, in more detail below. The heat flux into the coolant from the cathode plate is given by

$$Q_c = \kappa_p \frac{\theta_2 - \theta_1}{L_p} \quad (6)$$

and similarly from the anode plate is

$$Q_a = \kappa_p \frac{\theta_5 - \theta_1}{L_p}. \quad (7)$$

Here, L_p = 1mm is the plate thickness and κ_p =2.3 W/mºC. The total thermal flux density from the plates is $Q = Q_a + Q_c$. Each coolant channel (assumed circular of diameter d) has associated with it a section of MEA of width L_w (1.4 mm). Thus, the thermal flux density into the coolant is

$$\frac{QL_w}{\pi d}.$$

Now using standard conjugate heat transfer theory (Ozisik 1985) we obtain

$$\frac{QL_w}{\pi d} = Nu \frac{\kappa_o}{d}(\theta_1 - T) \quad (8)$$

where $T = T(y)$, the coolant temperature at the y location under consideration and κ_o =0.41 W/mºC. Note that the diameter of the coolant d cancels in this expression and does not influence the results.

Eqs. 3a, 3b, 4, 5, and 8 leads to a 5×5 system of linear equations for the reference temperatures $\underline{\theta}$. This involves the representation of $\theta(z)$ in terms of these reference values and leads to the correct profile. We show the results at three channel locations in Fig. 4 for the base membrane resistance case. These results are shown as offsets to the corresponding coolant temperatures. Cathode catalyst temperatures are shown in Fig. 5 for the three membrane resistances considered above. Note that the condensation term provides the most variation in local heat production. The sharp increase in cathode catalyst temperature near the inlet occurs where the gas channel saturates. Here, there is a discontinuous increase in MEA heating due to condensation. The coolant temperatures shown in Fig.1 see this discontinuity only in the derivative. The dip in cathode catalyst temperature at outlet due to the evaporative cooling has been observed experimentally.

STACK THERMAL MODEL

We begin the presentation of the stack model with a reformulation of the unit cell model above. Consider the thermal fluxes in Eqs. 6 and 7. In the unit cell case, it is known that $Q_c + Q_a$ is equal to the right hand side of Eq. 1 although in the stack case, the heat generated by one cell can be transferred to another cell's coolant. We consider an implicit discretization of Eq. 1 with the right hand side replaced by $Q_c + Q_a$. To update the temperature at the next point down the channel, the implicit discretization of Eq. 1 and the thermal balance equations Eqs. 3a, 3b, 4, 5, and 8 become a system of six linear equations for $\underline{\theta}$ and T at the next grid point down the channel.

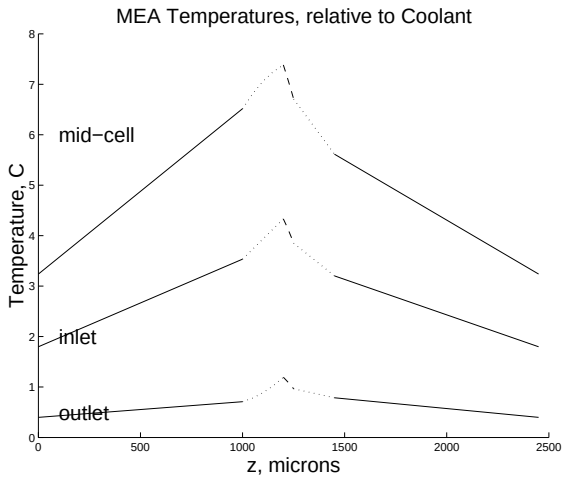

Fig. 4: Temperature through plates and MEA at three different channel locations (top is mid-cell, middle is inlet, bottom is outlet). The plate temperatures are shown with solid lines, the electrode temperatures are dotted and the membrane temperatures are dashed.

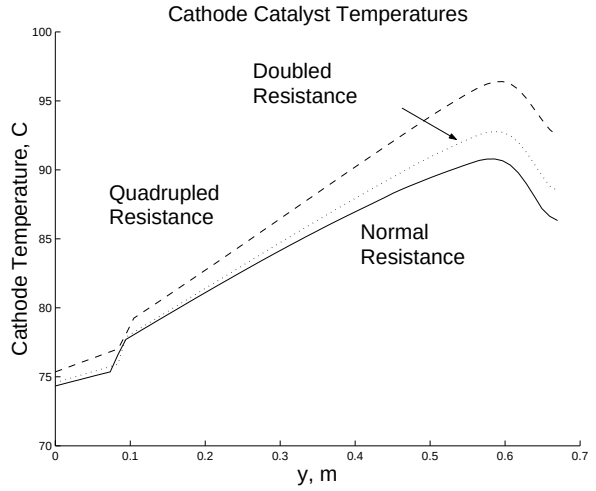

Fig. 5: Predicted cathode catalyst temperatures $\theta_3(y)$ for base membrane resistance (solid line), doubled resistance (dotted), quadrupled resistance (dashed).

It is now clear how to extend the model to the case of a stack with N cells. We have N copies of Eq. 1

$$cQ_o \frac{dT^j}{dy} = Q_a^{j-1} + Q_c^j \qquad (9)$$

where the superscript refers to cell number. We assume the stack ends are insulated. In each cell, we have the thermal balances Eqs. 3a, 3b, 4, 5, and 8. These and an implicit discretization of the vector Eq. 9 lead to a $6N \times 6N$ system of linear equations for the coolant temperatures and MEA reference temperatures in each cell at the next grid point down the channel.

We use this model to simulate the effect of one hot cell in a stack. We take a stack of N=15 cells running at base conditions except for the center cell whose membrane resistance is arbitrarily set to 4 times the base value so as to act as a localized source of additional heat. The temperature profiles down the cell are shown for the coolant (Fig. 6) and at the cathode catalyst (Fig. 7). The centre cell and three neighbours above it are shown. Note that the coolant channel "above" the anomaly is almost as hot as the anomalous cell (the solid and dashed lines in Fig. 6 almost overlap): in fact, these two coolant channels bracket the anomaly and so this is not surprising.

Note that the presence of the neighboring cells significantly reduces the heat increase of the hot cell: compare figures 6 to 1 and 7 to 5. A mathematical analysis of a model idealizing the MEA to an interface reveals that heat is spread to a characteristic number of cells that scales like

$$\sqrt{\frac{2L_c\kappa_p}{cQ_oL_p}} \approx 2.6$$

for the parameters used in this study. The analysis is that of uniform additional heating from a centre cell in an infinite stack and uses small argument approximations of Laplace transforms of the stack temperatures in the y variable. The details of this analysis will be shown in an upcoming publication.

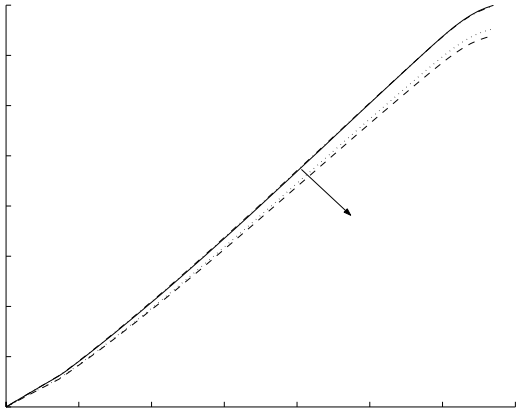

Fig. 6: Coolant temperatures in the stack. The anomalous hot cell is solid, first neighbour above is dot-dashed, second neighbour is dotted, and third neighbour is dashed.

SUMMARY

The authors have developed a simple thermal model of fuel cell stacks, using input from a previous model to provide estimates of heat generation in cells under different operating conditions. The effects of neighboring cells in regular operation next to an anomalously hot cell have been investigated. The simplicity of the model relies on the fact that straight-channel fuel cells are being modelled and that an averaging over the cross-channel direction x is appropriate.

A combined stack model that includes the coupling of temperature profiles provided by this model to performance is currently being developed in our group. We are also undertaking computational studies in the two-dimensional cross-plane $(x-z)$ with the correct geometry of gas and coolant channels to determine how accurate our average model is to this case. Experimental work to validate and fit the model to Ballard Mk9 hardware is under way.

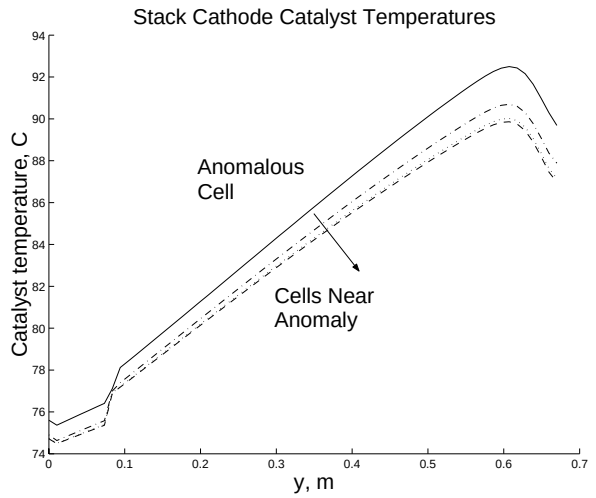

Fig. 7: Catalyst layer temperatures in the stack. The anomalous hot cell is solid, first neighbour above is dot-dashed, second neighbour is dotted, and third neighbour is dashed.

NOMENCLATURE

c	coolant heat capacity, J/kgºC.
H_{vap}	heat of vaporization, J/mole
$i(y)$	current density from unit cell model, A/m^2
L_c	channel length, m
L_g	electrode thickness, m
L_m	membrane thickness, m
L_p	plate thickness, m
L_w	MEA width per coolant channel, m
N	number of cells in stack model
Nu	Coolant Nusselt number, dimensionless
Q	$Q_a + Q_c$ combined heat flux to coolant, W/m^2
Q_a	Heat flux from anode to coolant, W/m^2
Q_c	Heat flux from cathode to coolant, W/m^2
$Q_l(y)$	cathode liquid water flux, moles/sm from unit cell model
Q_o	coolant flux, kg/sm
$R(y)$	area-specific membrane resistivity Ω-m^2 from unit cell model
$T(y)$	average coolant temperature, °C
V	cell voltage from unit cell model, V
V_a	anode endothermic voltage, V
V_{TN}	Thermal-Neutral voltage, V
x	cross-channel coordinate, m
y	down-channel coordinate, m
z	through-MEA coordinate, m
$\Gamma(y)$	condensation rate, moles/sm from unit cell model
$\eta(y)$	overpotential V
κ_g	thermal conductivity of electrodes, W/m°C
κ_m	thermal conductivity of membrane, W/m°C
κ_o	thermal conductivity of coolant, W/m°C
κ_p	thermal conductivity of plates, W/m/°C
$\theta(z)$	MEA temperature, °C
θ_1	plate temperature at coolant, °C
θ_2	plate temperature at cathode electrode, °C
θ_3	temperature of cathode catalyst, °C
θ_4	temperature of anode catalyst, °C
θ_5	plate temperature at anode electrode, °C

ACKNOWLEDGMENT

The authors thank the financial support of the MITACS NCE and Ballard Power Systems. We are grateful for the insight provided by Jean St-Pierre and Gwang-Soo Kim at Ballard.

REFERENCES

P. Berg, K. Promislow, J. St-Pierre, J. Stumper, and B. Wetton, 2004, Water management in PEM fuel cells, *Journal of the Electrochemical Society*, 151, pp. A341-A353.

T. Berning, D. Lu and N. Djilali, 2003, Three-dimensional computational analysis of transport phenomena in a PEM fuel cell – a parametric study, *J. Power Sources*, 124, pp. 440-452.

N. Djilali and D. M. Lu, 2002, Influence of heat transfer on gas and water transport in fuel cells, *International Journal of Thermal Science,* 41, pp. 29-40.

S. Dutta, S. Shimpalee, and J.W. Van Zee, 2001, Numerical prediction of mass exchange between cathode and anode channels in a PEM fuel cell, *Int. J. of Heat and Mass Transfer*, 44, pp. 2029-2042.

J. Larminie and A. Dicks, 2003, *Fuel Cell Systems Explained*, John Wiley and Sons, Ltd.

M. J. Lampinen and M. Famino, 1993, Analysis of Free Energy and Entropy Changes for Half-Cell Reactions, *J. Electrochem. Soc.,* 140, pp. 3537-3546.

S. Mazumder and J. V. Cole, 2003, Rigorous three-dimensional mathematical modeling of proton exchange membrane fuel cells. Part 1: Model predictions without liquid water transport, *J. Electrochem. Soc.,* 150, pp. A1503-A1509.

S. Mazumder and J. V. Cole, 2003, Rigorous three-dimensional mathematical modeling of proton exchange membrane fuel cells. Part 2: Model predictions with liquid water transport, *J. Electrochem. Soc.*, 150, pp. A1510-A1517.

D. Natarajan and T. Nguyen, 2003, Three-dimensional effects of liquid water flooding in the cathode of a PEM fuel cell, *J. Power Sources,* 115, pp. 66-80.

T. Nguyen and R. E. White, 1993, A water and heat management model for proton exchange membrane fuel cells, *Journal of Electrochemical Society,* 140, pp. 167-174.

M. N. Ozisik, 1985, *Heat Transfer: a Basic Approach*, McGraw-Hill, New York.

T. E. Springer, T. A. Zawodzinski and S. Gottesfeld, 1991, Polymer electrolyte fuel cell model, *J. Electrochem. Soc.*, 138, pp. 2334-2342.